

Acta Crystallographica Section F

**Structural Biology
and Crystallization
Communications**

ISSN 1744-3091

Expression, purification, crystallization and preliminary X-ray analysis of the receiver domain of *Staphylococcus aureus* LytR protein

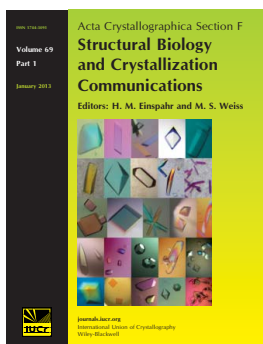
Agnesa Shala, Kevin H. Patel, Dasantila Golemi-Kotra and Gerald F. Audette

Acta Cryst. (2013). **F69**, 1418–1421

Copyright © International Union of Crystallography

Author(s) of this paper may load this reprint on their own web site or institutional repository provided that this cover page is retained. Reproduction of this article or its storage in electronic databases other than as specified above is not permitted without prior permission in writing from the IUCr.

For further information see <http://journals.iucr.org/services/authorrights.html>



Acta Crystallographica Section F: Structural Biology and Crystallization Communications is a rapid all-electronic journal, which provides a home for short communications on the crystallization and structure of biological macromolecules. Structures determined through structural genomics initiatives or from iterative studies such as those used in the pharmaceutical industry are particularly welcomed. Articles are available online when ready, making publication as fast as possible, and include unlimited free colour illustrations, movies and other enhancements. The editorial process is completely electronic with respect to deposition, submission, refereeing and publication.

Crystallography Journals **Online** is available from journals.iucr.org

**Agnesa Shala,^a Kevin H. Patel,^a
Dasantila Golemi-Kotra^{a,b*} and
Gerald F. Audette^{a,b*}**

^aDepartment of Chemistry, York University,
4700 Keele Street, Toronto, ON M3J 1P3,
Canada, and ^bDepartment of Biology,
York University, 4700 Keele Street, Toronto,
ON M3J 1P3, Canada

Correspondence e-mail: dgkotra@yorku.ca,
audette@yorku.ca

Received 7 October 2013

Accepted 11 November 2013



© 2013 International Union of Crystallography
All rights reserved

Expression, purification, crystallization and preliminary X-ray analysis of the receiver domain of *Staphylococcus aureus* LytR protein

The response-regulatory protein LytR belongs to a family of transcription factors involved in the regulation of important virulence factors in pathogenic bacteria. The protein consists of a receiver domain and an effector domain, which play an important role in controlled cell death and lysis. The LytR receiver domain (LytR^N) has been overexpressed, purified and crystallized using the sitting-drop and hanging-drop vapour-diffusion methods. The crystals grew as needles, with unit-cell parameters $a = b = 84.82$, $c = 157.3$ Å, $\alpha = \beta = 90$, $\gamma = 120^\circ$. LytR^N crystallized in space group $P6_122$ and the crystals diffracted to a maximum resolution of 2.34 Å. Based on the Matthews coefficient ($V_M = 5.44$ Å³ Da⁻¹), one molecule is estimated to be present in the asymmetric unit.

1. Introduction

Staphylococcus aureus is an opportunistic bacterial pathogen of significant concern owing to its ability to rapidly adapt to environmental conditions and to resist host innate immune defence mechanisms (Archer, 1998). The extensive use of antibiotics and the adaptability of *S. aureus* have led to the emergence of multidrug-resistant strains, such as methicillin-resistant *S. aureus* (MRSA; Ippolito *et al.*, 2010), in hospital and community settings. One of the major hurdles that *S. aureus* has to overcome during colonization of the host is the host's innate immune system. This defence mechanism relies on the release of numerous cationic antimicrobial peptides (CAMPs; Peschel, 2002; Voyich *et al.*, 2005). CAMPs are amphipathic peptides comprised of less than 50 amino acids and are found in most mammalian tissues (Brogden, 2005). They have bactericidal activity and their mechanism of action is proposed to involve perturbation of the cell membrane, which alters its electrical potential (Peschel *et al.*, 2001). The two-component system (TCS) LytSR has recently been proposed to function as a sense–response system for detecting subtle changes in the transmembrane potential of the cell (Patton *et al.*, 2006; Li *et al.*, 2007; Sharma-Kuinkel *et al.*, 2009).

LytSR is comprised of a membrane-bound sensor histidine kinase (HK) LytS and a response-regulator (RR) protein LytR. Recent studies have shown that LytS senses the decrease in transmembrane potential (Sharma-Kuinkel *et al.*, 2009), suggesting that the sensor kinase LytS may transduce this change in membrane potential intracellularly through phosphorylation of LytR. LytR is a transcription factor that regulates the *lrgAB* and *cidABC* operons (Brunskill & Bayles, 1996). Both operons are involved in the control of programmed cell death and cell lysis (Groicher *et al.*, 2000; Rice *et al.*, 2003). The gene products of the *cid* operon enhance murein hydrolysis activity (Rice *et al.*, 2003) and antibiotic tolerance, while the *lrg* genes inhibit these processes (Groicher *et al.*, 2000).

The RR protein LytR belongs to the AlgR/AgrA/LytR family of transcription factors (Sidote *et al.*, 2008) involved in the regulation of important virulence factors in pathogenic bacteria (Galperin, 2008). It consists of two domains, the N-terminal receiver domain (LytR^N) and the C-terminal effector domain (LytR^C). In general, the receiver domain of the RRs harbours a conserved Asp residue that undergoes reversible phosphorylation by the sensor histidine kinase (Gao *et al.*, 2007; Gao & Stock, 2010). It is generally accepted that phosphorylation of the receiver domain initiates a series of conformational changes that ultimately modulate the output response of the proteins

(Gao & Stock, 2010). LytR^C is a DNA-binding protein that falls into the novel family of non-helix–turn–helix DNA-binding domains known as LytTR (Nikolskaya & Galperin, 2002; Sidote *et al.*, 2008). The receiver domains are conserved among the different families of response regulators, OmpR and NarL , unlike the DNA-binding domain, which understandably needs to be variable in order to allow a specific response (Stock *et al.*, 2000; Gao *et al.*, 2007). Nonetheless, there is significant variability in the primary structures of receiver domains, which limits the cross-talk among two-component systems (Barbieri *et al.*, 2010). Understanding the structural and sequence elements that prevent cross-talk in TCS is paramount to understand specificity of signal transduction by these systems.

In the absence of structural studies on the LytR protein of *S. aureus*, and noting that full-length LytR forms highly insoluble aggregates upon concentration, we undertook crystallization of the LytR receiver domain (LytR^N ; residues 1–134). Noting that LytR^N shares sequence similarity with other structurally characterized TCS receiver domains such as CheY (Volz & Matsumura, 1991), NarL (Baikalov *et al.*, 1996) and OmpR (Solá *et al.*, 1999), which belong to different families, we are interested in comparing the structural aspects of these proteins. Here, we describe the expression, purification, crystallization and initial diffraction analysis of the receiver domain of LytR , LytR^N .

2. Materials and methods

2.1. Cloning and expression

The *lytR* gene (GenBank accession ID gi:1854577) was PCR-amplified from the MRSA strain Mu50 (ATCC 700699; Cedarlane) using the primers LytR-Dir , 5'-GGAATTCATATGAAAGCATTAATCATAGATGATG-3', and LytR-Rev , 5'-CGGAATTCTTATTAAAGTAATCCTATCGACG-3'. The primers were designed to contain *NdeI* and *EcoRI* restriction sites (italicized sequences) at the 5'- and 3'-ends of *lytR*, respectively. Following PCR amplification, the resulting 742 bp *lytR* amplicon was purified and both the PCR product and the pET-26b (Novagen) host vector were digested with *NdeI* and *EcoRI*. Subsequent ligation of *lytR* to pET-26b resulted in

the *pET26b::LytR* construct. The construct was used to transform *Escherichia coli* NovaBlue cells grown in medium supplemented with $50 \mu\text{g ml}^{-1}$ kanamycin (Kan) for amplification of the construct. The DNA sequence of *lytR* cloned into pET-26b was confirmed by DNA sequencing (The Centre for Applied Genomics, The Hospital for Sick Children, Toronto, Canada). To express only the receiver domain of the protein, LytR^N (residues 1–134), a stop codon was introduced after residue 134 using the QuikChange mutagenesis method (Agilent Technologies). Insertion of the stop codon was confirmed by DNA sequencing, resulting in vector *pET26b::LytR^N*. To express LytR^N , the *pET26b::LytR^N* vector was introduced into *E. coli* BL21 (DE3) cells. 1 ml of a 5 ml overnight culture containing a streak of the cells was used to inoculate 1 l Luria–Bertani (LB) broth supplemented with $50 \mu\text{g ml}^{-1}$ Kan. Cells were cultured at 310 K and 200 rev min^{-1} to mid-log phase ($\text{OD}_{600} = 0.5\text{--}0.7$). The culture was then cooled to 277 K prior to the induction of protein expression using 0.5 mM isopropyl β -D-1-thiogalactopyranoside (IPTG) at 298 K for 12 h. The cells were harvested by centrifugation at 3300g for 20 min at 277 K.

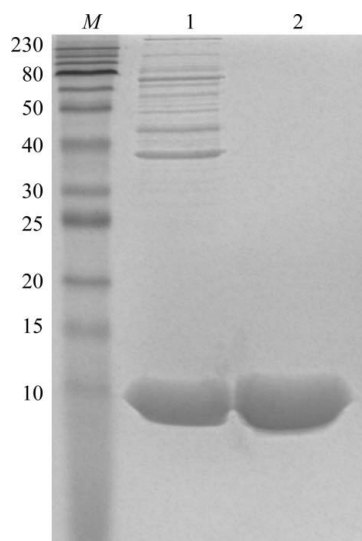
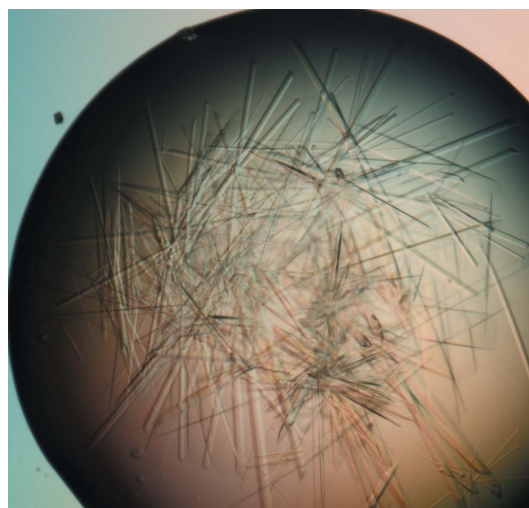
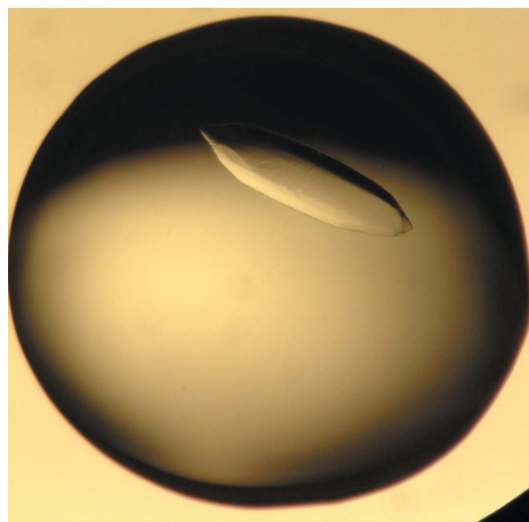


Figure 1 SDS-PAGE analysis of LytR^N purification. Lane *M*, molecular-weight marker (NEB; labelled in kDa); lane 1, purified LytR^N after isolation on a DEAE column; lane 2, 99% homogeneous LytR^N following size-exclusion chromatography used for crystallization.



(a)



(b)

Figure 2 Crystals of LytR^N . (a) Initial crystals grown from Crystal Screen 2 (Hampton Research) at 294 K; (b) an optimized LytR^N crystal with dimensions of $410 \times 166 \times 30 \mu\text{m}$ grown over a reservoir containing 0.1 M MES monohydrate pH 6.5, 1.6 M magnesium sulfate heptahydrate at 277 K.

2.2. Purification

To purify LytR^N, the cell pellet was resuspended in 1:10(*w*:*v*) buffer *A* (20 mM Tris pH 7.5, 5 mM MgCl₂). The resuspended cells were lysed by sonication (Sonic Dismembrator 500, Fisher Scientific) while cooling on ice for 5 min (10 s on/15 s off). The insoluble cell lysate was removed by centrifugation at 34 000*g* for 30 min at 277 K. The supernatant was loaded onto a pre-equilibrated 40 ml DEAE column (GE Healthcare) and the column was subsequently washed with at least five column volumes of buffer *A* to remove any contaminants. The bound protein was eluted over ten column volumes in a linear gradient to a final concentration of 100% buffer *B* (500 mM Tris pH 7.5, 5 mM MgCl₂) at a flow rate of 3 ml min⁻¹. LytR^N elution peaks were pooled and concentrated by centrifugation (1240*g* at 277 K) using an Amicon Ultra-3 concentrator (Millipore) to a final volume of 5 ml. LytR^N was then further purified and buffer-exchanged into buffer *C* (100 mM Tris pH 7.5, 5 mM MgCl₂) by size-exclusion chromatography on a HiPrep 26/60 Sephacryl S-200 HR gel-filtration column (GE Healthcare). Fractions corresponding to LytR^N were collected and concentrated to 13 mg ml⁻¹ prior to crystallization. The homogeneity of the protein was determined by Coomassie Blue staining of an 18% SDS polyacrylamide gel (Fig. 1). The identity of the protein was confirmed by in-gel trypsin digestion (Sigma) and mass-spectrometric analysis (Advanced Protein Technology Centre, Toronto). The molecular mass of the protein was determined to be 15 027 Da by electrospray ionization mass spectrometry (ESI-MS), which matches the sequence predicted mass of 15 028 Da.

2.3. Crystallization

Initial crystallization experiments were performed by screening conditions from the commercially available kits Crystal Screen and Crystal Screen 2 from Hampton Research (Jancarik & Kim, 1991) and The JCSG Core Suite II from Qiagen (Lesley & Wilson, 2005). The trials were set up in 96-well sitting-drop plates (Axygen) by hand with 1 μl protein solution (6–13 mg ml⁻¹) and mother liquor in a 1:1

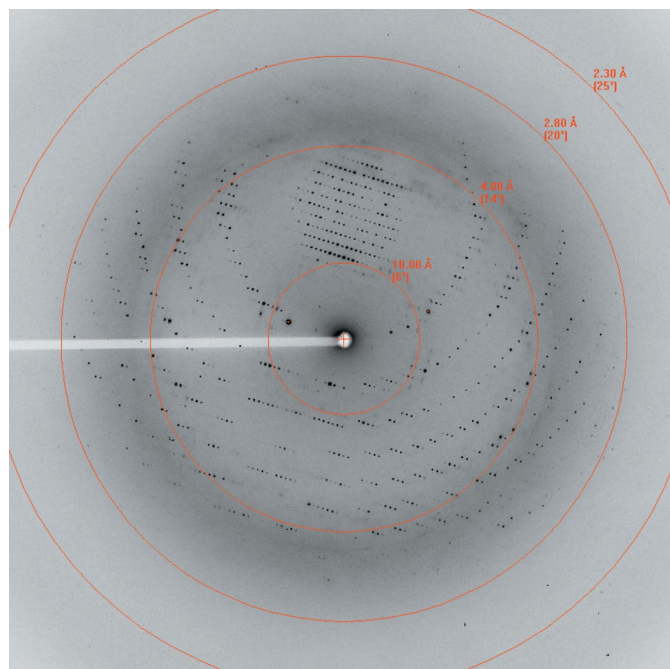


Figure 3
Diffraction image of a LytR^N crystal. Resolution rings correspond to 10.0, 4.0, 2.8 and 2.3 Å, respectively.

Table 1

Data-collection statistics.

Values in parentheses are for the outer shell.

Space group	<i>P</i> 6 ₁ 22
Unit-cell parameters (Å, °)	<i>a</i> = <i>b</i> = 84.82, <i>c</i> = 157.3, α = β = 90, γ = 120
Resolution range (Å)	66.56–2.34 (2.44–2.34)
Total No. of reflections	310181 (32139)
No. of unique reflections	14816 (1619)
Completeness (%)	100 (100)
Average <i>I</i> /σ(<i>I</i>)	14.3 (1.5)
<i>R</i> _{merge} †	0.111 (2.508)
<i>R</i> _{meas} ‡	0.114 (2.573)
<i>R</i> _{p.i.m.} §	0.025 (0.571)
CC _{1/2}	0.997 (0.937)
Multiplicity	20.9 (19.9)
Mosaicity (°)	0.37

† $R_{\text{merge}} = \frac{\sum_{hkl} \sum_i |I_i(hkl) - \langle I(hkl) \rangle|}{\sum_{hkl} \sum_i I_i(hkl)}$. ‡ $R_{\text{meas}} = \frac{\sum_{hkl} \{ [N(hkl) / (N(hkl) - 1)]^{1/2} \sum_i |I_i(hkl) - \langle I(hkl) \rangle| \}}{\sum_{hkl} \sum_i I_i(hkl)}$. § $R_{\text{p.i.m.}} = \frac{\sum_{hkl} \{ [1 / (N(hkl) - 1)]^{1/2} \sum_i |I_i(hkl) - \langle I(hkl) \rangle| \}}{\sum_{hkl} \sum_i I_i(hkl)}$, where $I_i(hkl)$ and $\langle I(hkl) \rangle$ represent the diffraction intensity values of the individual measurements and the corresponding mean values, respectively.

ratio over a reservoir containing 70 μl mother liquor. The crystal trays were stored at 294 K. These trials yielded a number of hits producing numerous thin needle-like crystals (Fig. 2*a*) from various conditions, most of which contained ammonium or lithium sulfate as the precipitant, within 1 d. The best crystals were obtained from 0.1 M MES monohydrate pH 6.5, 1.6 M magnesium sulfate heptahydrate. Optimization of the crystallization conditions was performed by varying the precipitant concentration and the buffer pH using hanging-drop EasyXtal 15-well plates with drop-guard crystallization supports (Qiagen) and incubating the plates at a lower temperature of 277 K. The best diffracting crystals grew using 7 mg ml⁻¹ protein solution mixed with an equal amount of reservoir solution (0.1 M MES monohydrate pH 6.5, 1.6 M magnesium sulfate heptahydrate) equilibrated against 0.5 ml reservoir solution at 277 K over 6 d. The single crystals grew into rods with maximum dimensions of 410 × 166 × 10 μm (Fig. 2*b*).

2.4. Data collection

To prepare the crystals for data collection, they were cryoprotected by soaking them directly in a new drop of mother liquor supplemented with 20%(*v*/*v*) glycerol for 45–60 s prior to vitrification in liquid nitrogen. Crystals were screened in-house using Cu *K*α X-ray radiation on a MicroMax-007 HF rotating-anode generator with a Saturn 944+ CCD detector (Rigaku) prior to shipping to the Canadian Macromolecular Crystallography Facility (CMCF) at the Canadian Light Source (CLS). X-ray diffraction data were collected on CMCF beamline 08ID-1 at 100 K: 240 images of 0.75° φ oscillation per frame were collected on an MX 300 CCD detector with a 340 mm crystal-to-detector distance and an exposure time of 1.0 s per image. The data were processed using *MOSFLM* (Leslie & Powell, 2007) and were integrated and scaled using *AIMLESS* and *CTRUNCATE* (Evans, 2011; Padilla & Yeates, 2003) from the *CCP4* program suite (Winn *et al.*, 2011).

3. Results

The receiver domain of LytR, LytR^N, has been expressed and purified to homogeneity (Fig. 1). The yield of pure protein was 26 mg per litre of culture. Purified LytR^N concentrated to 7 mg ml⁻¹ yielded crystals belonging to space group *P*6₁22, with unit-cell parameters *a* = *b* = 84.82, *c* = 157.3 Å, α = β = 90, γ = 120°, that diffracted to 2.34 Å resolution

(Fig. 3). No evidence of radiation damage was observed in the diffraction images over the course of data collection, and the data-collection statistics are summarized in Table 1. While the average $I/\sigma(I)$ dropped below 2.0 beyond 2.44 Å resolution, $CC_{1/2}$ analysis in *AIMLESS* indicated that true resolution of the crystal was 2.34 Å, despite an average $I/\sigma(I)$ of 1.5 in the 2.44–2.34 Å high-resolution shell (Table 1). Cell-content calculations (Matthews, 1968) predict that each asymmetric unit contains one monomer of LytR^N ($V_M = 5.44 \text{ \AA}^3 \text{ Da}^{-1}$) with 77.39% solvent. Structure solution and refinement are ongoing using molecular replacement with AF1382 (PDB entry 2qvo; Southeast Collaboratory for Structural Genomics, unpublished work) as the search model, to which LytR^N is predicted to have a similar secondary structure and 37% sequence similarity using *Phyre*² (Kelley & Sternberg, 2009).

This research was supported by grants from the Natural Sciences and Engineering Council of Canada (NSERC; to GFA and DGK), the Canadian Foundation for Innovation (CFI), the Early Researcher Award Program (to DGK) from the Ministry of Economic Development and Innovation (Ontario, Canada) and York University. Data collection described in this paper was performed at the Canadian Light Source, which is funded by the CFI, NSERC, the National Research Council Canada, the Canadian Institutes of Health Research, the Government of Saskatchewan, Western Economic Diversification Canada and the University of Saskatchewan.

References

- Archer, G. L. (1998). *Clin. Infect. Dis.* **26**, 1179–1181.
- Baikalov, I., Schröder, I., Kaczor-Grzeskowiak, M., Grzeskowiak, K., Gunsalus, R. P. & Dickerson, R. E. (1996). *Biochemistry*, **35**, 11053–11061.
- Barbieri, C. M., Mack, T. R., Robinson, V. L., Miller, M. T. & Stock, A. M. (2010). *J. Biol. Chem.* **285**, 32325–32335.
- Brogden, K. A. (2005). *Nature Rev. Microbiol.* **3**, 238–250.
- Brunskill, E. W. & Bayles, K. W. (1996). *J. Bacteriol.* **178**, 5810–5812.
- Evans, P. R. (2011). *Acta Cryst.* **D67**, 282–292.
- Galperin, M. Y. (2008). *Structure*, **16**, 657–659.
- Gao, R., Mack, T. R. & Stock, A. M. (2007). *Trends Biochem. Sci.* **32**, 225–234.
- Gao, R. & Stock, A. M. (2010). *Curr. Opin. Microbiol.* **13**, 160–167.
- Groicher, K. H., Firek, B. A., Fujimoto, D. F. & Bayles, K. W. (2000). *J. Bacteriol.* **182**, 1794–1801.
- Ippolito, G., Leone, S., Lauria, F. N., Nicastrì, E. & Wenzel, R. P. (2010). *Int. J. Infect. Dis.* **14**, Suppl. 4, S7–S11.
- Jancarik, J. & Kim, S.-H. (1991). *J. Appl. Cryst.* **24**, 409–411.
- Kelley, L. A. & Sternberg, M. J. E. (2009). *Nature Protoc.* **4**, 363–371.
- Lesley, S. A. & Wilson, I. A. (2005). *J. Struct. Funct. Genomics*, **6**, 71–79.
- Leslie, A. G. W. & Powell, H. R. (2007). *Evolving Methods for Macromolecular Crystallography*, edited by R. J. Read & J. L. Sussman, pp. 41–51. Dordrecht: Springer.
- Li, M., Lai, Y., Villaruz, A. E., Cha, D. J., Sturdevant, D. E. & Otto, M. (2007). *Proc. Natl Acad. Sci. USA*, **104**, 9469–9474.
- Matthews, B. W. (1968). *J. Mol. Biol.* **33**, 491–497.
- Nikolskaya, A. N. & Galperin, M. Y. (2002). *Nucleic Acids Res.* **30**, 2453–2459.
- Padilla, J. E. & Yeates, T. O. (2003). *Acta Cryst.* **D59**, 1124–1130.
- Patton, T. G., Yang, S.-J. & Bayles, K. W. (2006). *Mol. Microbiol.* **59**, 1395–1404.
- Peschel, A. (2002). *Trends Microbiol.* **10**, 179–186.
- Peschel, A., Jack, R. W., Otto, M., Collins, L. V., Staubitz, P., Nicholson, G., Kalbacher, H., Nieuwenhuizen, W. F., Jung, G., Tarkowski, A., van Kessel, K. P. & van Strijp, J. A. (2001). *J. Exp. Med.* **193**, 1067–1076.
- Rice, K. C., Firek, B. A., Nelson, J. B., Yang, S.-J., Patton, T. G. & Bayles, K. W. (2003). *J. Bacteriol.* **185**, 2635–2643.
- Sharma-Kuinkel, B. K., Mann, E. E., Ahn, J.-S., Kuechenmeister, L. J., Dunman, P. M. & Bayles, K. W. (2009). *J. Bacteriol.* **191**, 4767–4775.
- Sidote, D. J., Barbieri, C. M., Wu, T. & Stock, A. M. (2008). *Structure*, **16**, 727–735.
- Solá, M., Gomis-Rüth, F. X., Serrano, L., González, A. & Coll, M. (1999). *J. Mol. Biol.* **285**, 675–687.
- Stock, A. M., Robinson, V. L. & Goudreau, P. N. (2000). *Annu. Rev. Biochem.* **69**, 183–215.
- Volz, K. & Matsumura, P. (1991). *J. Biol. Chem.* **266**, 15511–15519.
- Voyich, J. M., Braughton, K. R., Sturdevant, D. E., Whitney, A. R., Said-Salim, B., Porcella, S. F., Long, R. D., Dorward, D. W., Gardner, D. J., Kreiswirth, B. N., Musser, J. M. & DeLeo, F. R. (2005). *J. Immunol.* **175**, 3907–3919.
- Winn, M. D. *et al.* (2011). *Acta Cryst.* **D67**, 235–242.